CoSalen-Catalyzed Radical Hydrofunctionalization of Unactivated Internal Olefins at Low Catalyst Loading: Method Development, Regioselectivity, and Applications in Post-Polymerization Modification

Yun-Nian Yin, Bang-Sen Zhao, Han-Yuan Liu, Rui-Qing Sheng, Dong-Chen Ouyang and Rong Zhu*

Beijing National Laboratory of Molecular Sciences (BNLMS), Key Laboratory of Bioorganic Chemistry and Molecular Engineering of Ministry of Education, College of Chemistry and Molecular Engineering, Peking University, Beijing 100871, China

**corresponding author, e-mail: rongzhu@pku.edu.cn*

Abstract: The past two decades witnessed the rapid development of CoSalen-catalyzed hydrofunctionalization reactions, mostly on terminal and conjugation-activated olefins. However, the use of 1,2-dialkylsubstituted alkenes continues to pose challenges. In this study, we revisit this substrate class in the context of Carreira-type hydrofunctionalization reactions and introduce a simple yet effective modification (over 250-fold-increase in TON). Near-quantitative yields can be achieved at a low catalyst loading, typically 0.05 mol%. The key lies in inhibiting the degradation of the Salen backbone using molecular sieves. This new protocol facilitates a study on the MHAT regioselectivity of this type of alkenes. We found that allylic electron-negative groups and hyperconjugation have profound effects, yielding regioisomeric ratios ranging from 6.5:1 to < 1:20. The high TON, mild conditions, and versatility of this method further enable its application in the post-polymerization modification of several olefin-rich, commodity-relevant polymers.

Olefin hydrofunctionalization via metal hydride hydrogen atom transfer (MHAT) has evolved into a highly versatile and useful synthetic tool.[1,2] The pioneering works of Mukaiyama and Drago introduced cobalt(III) complexes, supported by weak-field ligands, for catalytic hydration.[3,4] A general Co-catalyzed hydrofunctionalization method, employing various radicalophiles, was established by Carreira in the mid-2000s, which set the stage for numerous subsequent developments (Figure 1a).[5-12] Recent advances in this field involve exploring the oxidative functionalization pathway via organocobalt(IV)[13-20] and electrochemical[21-24] or photochemical[25-28] generation of active cobalt hydride species. Most of these reactions utilize a salicylaldehyde-ethylenediamine-derived planar tetradentate ligand for cobalt (CoSalen).

In contrast to the fruitful expansion of the chemical space preceding and following the MHAT step, it is noteworthy that the majority of CoSalen-catalyzed examples deal with terminal and conjugation-activated internal olefins. Alkyl-substituted internal alkenes are much less reactive, particularly 1,2-dialkylsubstituted ones due to both steric hindrance and lack of extra radical stabilization.[2,29-31] Interestingly, their "MHAT inertness", at least under typical conditions, has enabled several synthetically useful transformations, such as kinetically controlled alkene migration,[32-34] alkyne semi-reduction,[23] and chemoselective hydroamidation.[35]

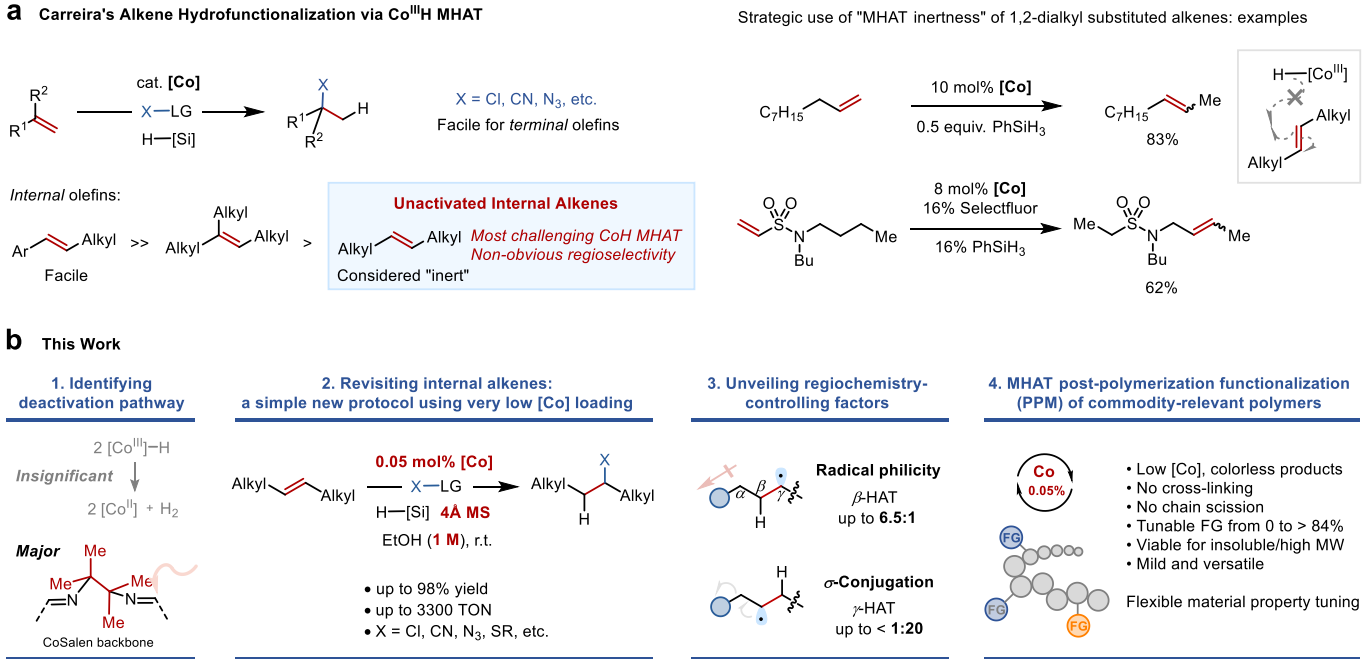

Figure 1 | Revisiting unactivated internal olefins in CoSalen-catalyzed MHAT hydrofunctionalizations.

The catalytic hydrofunctionalization of unactivated internal olefins in general is a challenging and important class of transformations, with 3d metal-based solutions being particularly attractive.[36-38] Besides this, our own motivation to revisit these substrates is two-fold. Firstly, they are prevalent in commodity-relevant polymer backbones such as polybutadienes and polynorbornenes.[39-42] The ability to functionalize these double bonds, ideally at very low Co loading, could enable value-added materials with tunable properties that are difficult to access via polymerization of functionalized monomers.[43,44] In this context, the metalloradical nature of Co(II) could serve to inhibit chain scission or cross-linking often encountered in traditional radical chemistry.[45] Secondly, the MHAT regioselectivity of unsymmetrical 1,2-dialkylsubstituted alkenes largely remains elusive. We believe that an investigation into this issue could reveal hidden factors usually overwhelmed by the Markovnikov selectivity.

Here we wish to report a simple yet surprisingly effective modification of the Carreira-type hydrofunctionalization, which allows for up-to-quantitative conversion of 1,2-dialkylsubstituted olefins using only 0.05 mol% CoSalen (Figure 1b). The key is identifying the main deactivation pathway, namely the hydrolytic degradation of the Salen backbone. This can be mitigated by simply adding molecular sieves, which leads to over 250-fold-increase in turnover numbers (TON). This new protocol facilitated a structure-selectivity study, unveiling the roles of allylic groups in determining the regiochemical outcome of putative MHAT. We further translated this protocol into a new post-polymerization modification (PPM) method for several commodity-relevant high molecular weight (MW) polymers, demonstrating the rich potential of MHAT hydrofunctionalization in macromolecular settings.

We began our investigation by evaluating the catalyst performance in the Carreira hydrochlorination reactions of 1,2-dialkylsubstituted olefins.[8] To this, 7-tetradecene (**1a**) was treated with tosyl chloride, phenylsilane, and 5 mol% [Co] (**C1**-**4**) in ethanol ($[\mathbf{1a}]_0$ = 0.2 M) at ambient temperature (Figure 2a). A clean, albeit low, conversion of **1a** to the hydrochlorination product **2a** was observed in the latter three cases. **C4**, which bears a benzenediamine-derived salen backbone, provided the best conversion (~ 50%). Interestingly, the kinetic profiles suggest that the initial rate follows a different trend. **C2** emerged as the most active catalyst, affording substantial conversion within the first 10 min. However, it suffered from severe catalyst deactivation, resulting in a lower final conversion compared to **C4**, which is less active but more persistent. This observation implied that effectively stabilizing **C2** could be key to addressing the internal alkene problem.

A commonly suggested deactivation pathway is the accumulation of Co(II) species due to bimolecular H_2 evolution via cobalt hydride.[46] We analyzed the reaction headspace by gas chromatography (Figure 2b). While H_2 was consistently detected across various reaction concentrations for **C4**, the more active catalyst **C2** did not yield a detectable amount of H_2 until the concentration was elevated (5 mol% at $[\mathbf{1a}]_0$ = 0.5 M). Meanwhile, monitoring the reaction by UV-Vis spectroscopy revealed backbone degradation of **C2** (Figure 2d, red trace, λ_{max} ~ 345 nm). This led to the proposal that for **C2** at low concentrations, hydrolytic decomposition of the salen backbone, rather than bimolecular H_2 evolution, seems to be the major cause for the loss of catalytic activity (Figure 2d). On the other hand, **C4**'s aromatic imine backbone is more resistant to hydrolytic cleavage, which is consistent with its observed persistency. In this regard, Holland recently suggested a bimetallic reduction pathway involving a [Co]−H and $[Co]^+$ species that releases a proton.[20] Such a Co-catalyzed acid-forming process could account for the rapid backbone hydrolysis after the early stage.

While a base might mitigate this problem, it is known that [Co]−H can be readily deprotonated by moderate bases such as amines. Excess silaphilic bases may add to the complication by overly activating the silane in an uncontrolled manner to produce H_2. Therefore, we turned to molecular sieves (MS) as simple, inexpensive, and innocent scavengers for both trace acid and moisture (Figure 2e).[47] Simply adding 4Å MS led to a dramatic boost to over 95% conversion using 5 mol% **C2** (Table S4). It was subsequently found that essentially quantitative yield was achieved using only 0.03 mol% **C2**, corresponding to > 3,300 TON. For comparison, in the absence of MS, the TON was merely 6-8, and the conversion below 0.5 mol% catalyst loading was actually too small to measure.

At this point, we revisited the kinetics of the model reaction (Figure 2f). At 0.05 mol% loading in the presence of MS, **C2** provided a remarkable 94% conversion within 1 h. It is worth noting that such low [Co] loading also allowed for concentrating the reaction without significant H_2 evolution ($[\mathbf{1a}]_0$ = 1.0 M), which is advantageous for potential scaling-up applications due to reduced waste and time consumption. Suppressing the catalyst decomposition enables a more accurate kinetic analysis of the entire reaction course. The rate showed 0^{th} order dependence in tosyl chloride, and an apparent mixed order dependence in [**1a**] (Figures S3 and S4). The latter could be attributable to a transition from 0^{th} to 1^{st} order as [**1a**] decreases, corresponding to a shift of turnover-limiting step to HAT after the initial

stage.[20,48] As expected, MS also improved the performances of **C3** and **C4** to different extends, reflecting their respective stabilities.

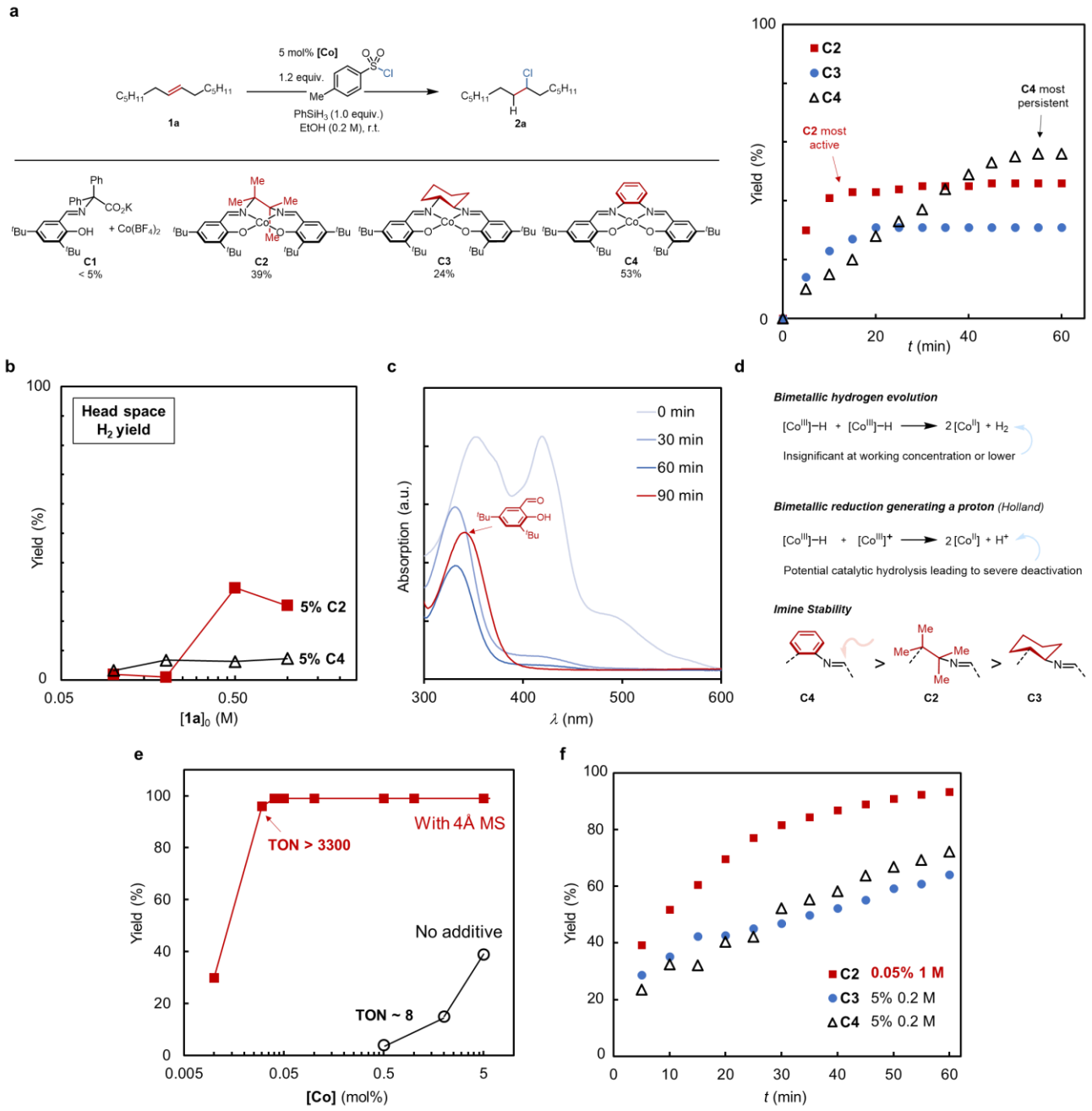

Figure 2 | **Model reaction study. a.** Catalyst performance evaluation in the hydrochlorination reaction under the original literature conditions[8]. **b-d.** Identifying catalyst backbone degradation as the most probable deactivation pathway. **e.** The addition of 4Å MS dramatically increases the reaction efficiency. **f.** Kinetic profiles in the presence of MS. **1a** (1.0 mmol), TsCl (1.2 mmol), $PhSiH_3$ (1.0 mmol), 4Å MS (200 mg) at r.t. ■: 0.05 mol% **C2** in 1.0 mL EtOH. ●: 5 mol% **C3** in 2.5 mL EtOH. Δ: 5 mol% **C4** in 2.5 mL EtOH. All yields were determined by gas chromatography. See supporting information for detail.

With the optimal protocol in hand, we examined the hydrochlorination reaction of a range of unactivated internal alkenes at 0.05 mol% catalyst loading (Figure 3a). Excellent isolated yields were obtained for acyclic and macrocyclic substrates (**2a-d**). Useful functional groups such as sulfonates, *N*-Boc, silyl ethers, benzyl ethers, and heterocycles were well tolerated (**2e-j**). No alkene migration or cycloisomerization with an adjacent phenyl group (**2b**) was detected, indicating fast trapping of the radical intermediate by chlorination.

Unlike terminal alkenes and styrene derivatives, regioselectivity prediction is not straightforward for an unsymmetrical dialkyl-substituted alkene. This is because its reaction with a putative [Co]−H could yield two regioisomeric 2° alkyl radicals of similar stabilities. However, this could make unactivated internal alkenes a unique mechanistic lens to unveil subtle features of the elusive MHAT step, experimentally. Literature data describing the regioselectivity of such substrates is especially scarce, presumably due to their low MHAT reactivity. Our new protocol enables an investigation of this issue (Figure 3b). Specifically, we selected substrates bearing different allylic (noted as α) substituents, and the products were analyzed for ratios of HAT to the β vs. γ-carbon. This ratio was found insensitive to an α-methyl branching, and the transfer of an H atom to the less hindered γ-carbon was only slightly favored (**1k**, β : γ = 1:2.2). Allylic halides displayed interesting divergent selectivities. The strongly electron-negative fluorine directs β-HAT (**1l**, β : γ = 6.5:1), presumably due to the electrophilicity of [Co]−H species that favors the formation of a more nucleophilic 2° radical. An allylic iodide, on the contrary, gave exclusive γ-HAT (**1m**, β : γ < 1:20). This might be attributable to the weak and polarizable C−I bond that provides effective spin delocalization in the transition state. The resulting β-iodoalkyl radical readily fragmentates to reveal a terminal alkene that is functionalized again *in situ*, thereby giving **3m/3m′** as the sole isolable products in place of the normal hydrochlorination.

A mechanistic proposal is depicted to explain the observed products derived from γ-HAT (Figure 3c). It is noteworthy that for groups incapable of radical fragmentation, elimination is still operational. For instance, **3l** was detected (~1%) under the standard conditions, and its yield substantially increased to 8% in the absence of MS. This could be reminiscent of β-elimination of an alkylcobalt complex, which can be facilitated by a proton.[49] Consistent with this hypothesis, MS has little effect in the allyl iodide case, as it eliminates via the radical directly.[50] The analysis of a D-labeling experiment actually benefited from the Co-mediated elimination pathway due to simplified isolation. The identification of **2n-β-**d_1 without D-scrambling confirmed that the MHAT step is indeed kinetically controlled (Figure 3d). As a side note, given the complex product distribution, we recommend careful analysis based on a proper mass balance to avoid overestimation of MHAT regioselectivity, especially in allylic systems.

To gain a more quantitative understanding, we collected additional examples and modeled the regioselectivity trend by multivariate linear free energy relationship (Figure 3e).[51] We selected two parameters, namely the group electron negativity (χ) and the computed thermodynamic energy difference between the regioisomeric radicals ($\Delta\Delta G_{\beta\gamma}$), to describe the electron-withdrawing and hyperconjugation effects of the allylic substituents, respectively.[52] While either parameter alone does not afford a satisfying result (R^2 = 0.6-0.8), the two-variate-linear-regression fitting provides an excellent correlation (R^2 = 0.98) and thus validating our analysis on the main factors controlling MHAT regiochemistry. Meanwhile, contributions from steric effect and chelation seem insignificant (OTBS vs. OH/F).

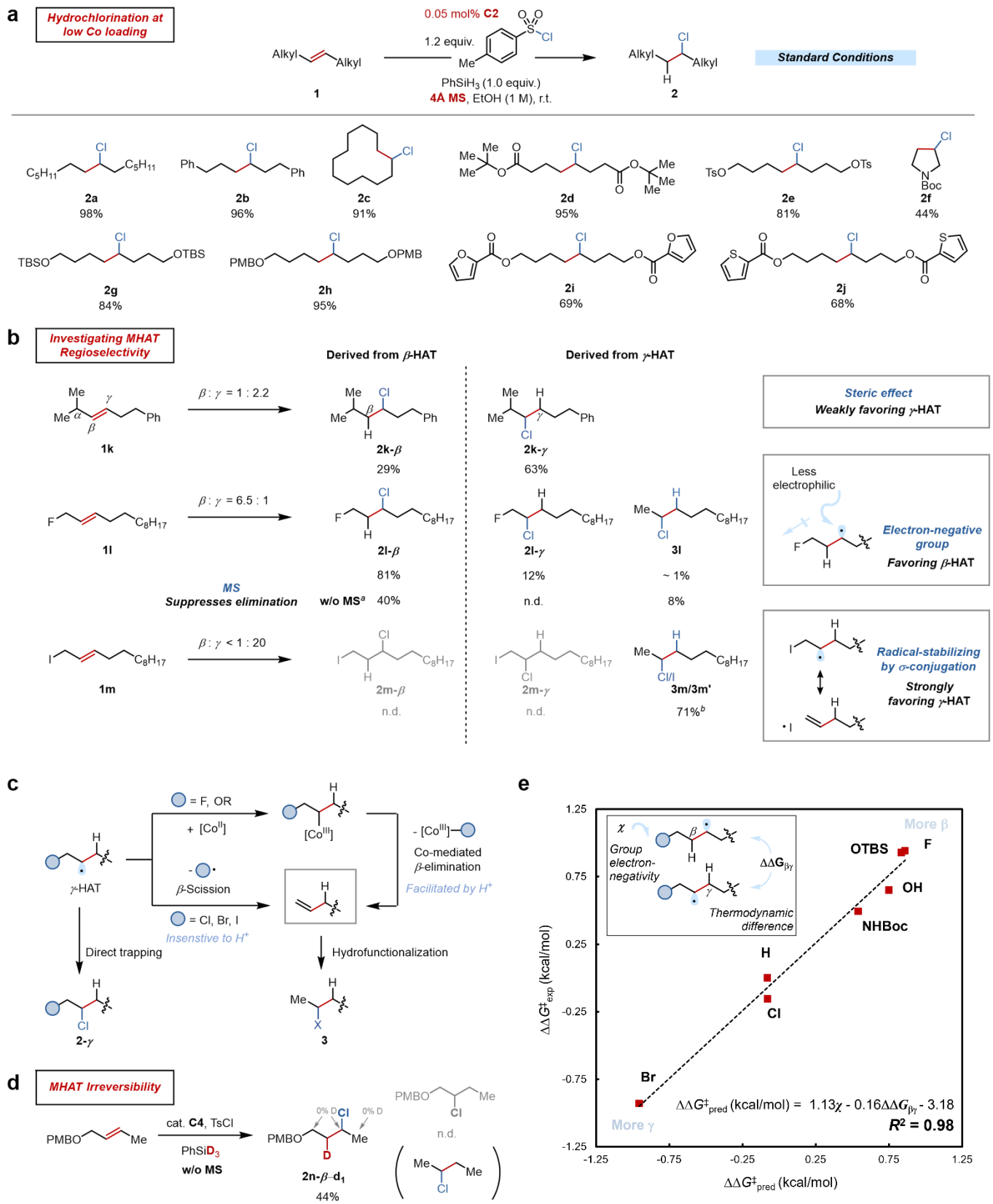

Figure 3 | Scope and regioselectivity in the hydrochlorination reactions of 1,2-dialkyl olefins. a. Scope of symmetrical 1,2-dialkyl olefins. Isolated yields. *Standard conditions*: **1** (0.50 mmol), **C2** (0.05 mol%), TsCl (0.60 mmol), $PhSiH_3$ (0.50 mmol), 4Å MS (100 mg) in 0.5 mL EtOH at r.t. for 12 h. **b.** Regioselectivity of unsymmetrical substrates. [a]w/o MS, **C2** (10 mol%) was used. [b]**C4** (10 mol%) was used in place of **C2**. Regioisomeric ratios were determined by ^{1}H NMR analysis of the crude reaction mixture. **c.** Mechanistic hypothesis of downstream pathways of γ-HAT. **d.** Deuterium labeling experiment. **e.** Multivariate linear regression modelling of the regioselectivity as a function of group electron negativity (χ) and DFT-computed (B3LYP/def2TZVP) thermodynamic energy difference between the regioisomeric radicals ($\Delta\Delta G_{\beta\gamma}$)

https://doi.org/10.26434/chemrxiv-2024-bf64r **ORCID:** https://orcid.org/0000-0001-5035-3531

Given the broad scope of radicalophiles that have already been demonstrated in the Carreira-type hydrofunctionalization reactions, we proceeded to install other useful functional groups such as azide, cyanide, thioethers under the standard conditions (Figure 4, **4a-k**). Mukaiyama oxidation at low catalyst loading was also demonstrated (**4l-m**). High TONs (~1000) were consistently obtained, paving the way toward versatile post-polymerization modifications. However, we note that the current modification, unfortunately, does not enable the CoSalen-catalyzed oxidative hydrofunctionalizations of 1,2-dialkyl olefins, where the catalyst stability seems not the limiting factor and thus alternative approaches are being investigated (Figure S7).

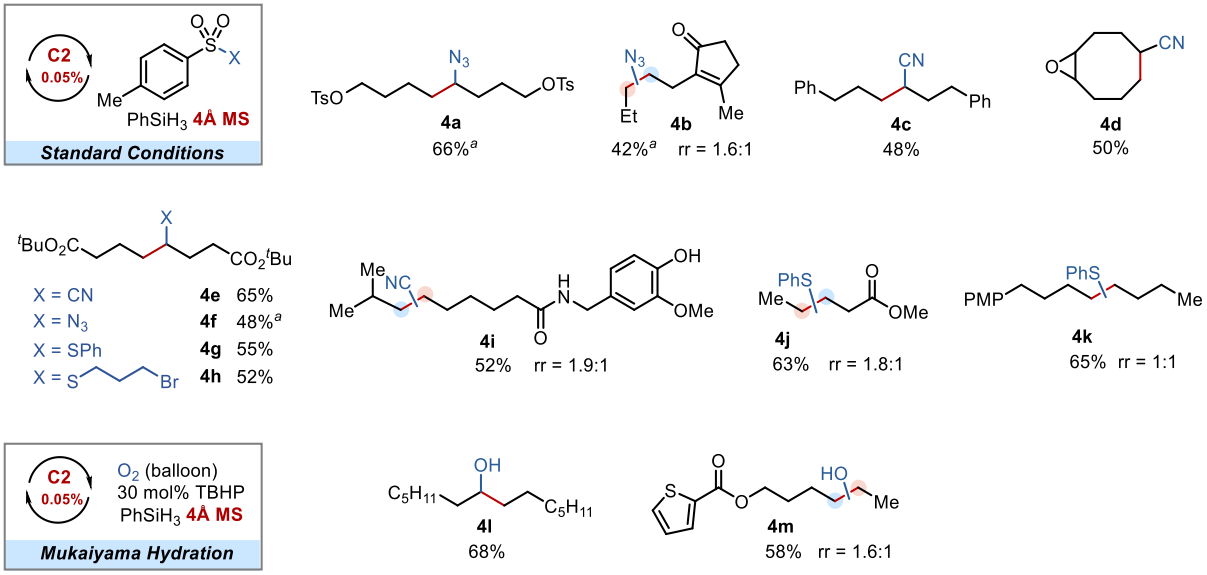

Figure 4 | Hydrofunctionalization using alternative radicalophiles. *Standard conditions:* alkene (0.50 mmol), **C2** (0.05 mol%), Ts−X (0.60 mmol), $PhSiH_3$ (0.50 mmol), 4Å MS (100 mg) in 0.5 mL EtOH at r.t. for 12 h. For hydration, O_2 (balloon pressure) and 30 mol% *tert*-butyl hydrogen peroxide (TBHP) were used in place of TsX. ●: The major site of C−X formation. [a]**C2** (0.10 mol%) was used.

In the final part of this work, we focus on translating the highly efficient small molecule reactions into a protocol for the controlled modification of several commodity-relevant polymer skeletons. Polynorbornenes produced by ring-opening metathesis polymerization (ROMP) are inherently rich in internal olefins. Functionalizing these double bonds leads to an increased glass transition temperature (T_g), which is desirable for high gas permeability membrane materials.[53] In this context, we subjected polynorbornene **P1** to the standard protocol (0.05 mol% **C2** with respect to the number of double bonds) and observed smooth hydrochlorination at room temperature (Figure 5a). No cross-linking or chain-scission was detected in the gel permeation chromatography (GPC) traces after modification. ^{1}H NMR spectroscopy of the products **P1-Cl** revealed a tunable degree of functionalization across 0 to 56% as a function of the stoichiometry of tosyl chloride ranging from 0 to 1.2 equivalents. These numbers were in line with the mass loss during the first decomposition event (at ca. 270 °C) found in thermogravimetric analysis (TGA). The samples of **P1-Cl** were studied by differential scanning calorimetry (DSC). A steady increase of T_g was found as the degree of functionalization increased, demonstrating effective modulation of polynorbornene's thermal property by simply varying the reagent stoichiometry.

High efficiency alone does not guarantee the successful translation of small molecule reactions to PPM methods. A major challenge is the low solubility of macromolecules, especially the more interesting high MW ones. To examine this issue in our system, a sample of **P1** (70.4 kg/mol, $Đ$ = 2.0) was prepared and found indeed insoluble in the reaction medium (1 M EtOH/CH_2Cl_2, corresponding to 152 mg/mL). To our surprise, it was found that the heterogeneity did not impede the PPM (Figure 5b). This could be, at least in part, attributed to the persistency of the catalyst. Hydrochlorination took place without any assistance by heating or dilution, and afforded **P1-Cl** in 64% degree of functionalization. In fact, we observed that the original polymer chunk sitting at the bottom of the reaction vessel gradually dissolved while the reaction proceeded, as the functionalization improved solubility. Therefore, we have demonstrated that this Co-catalyzed protocol is amenable for certain high MW materials with limited solubility.

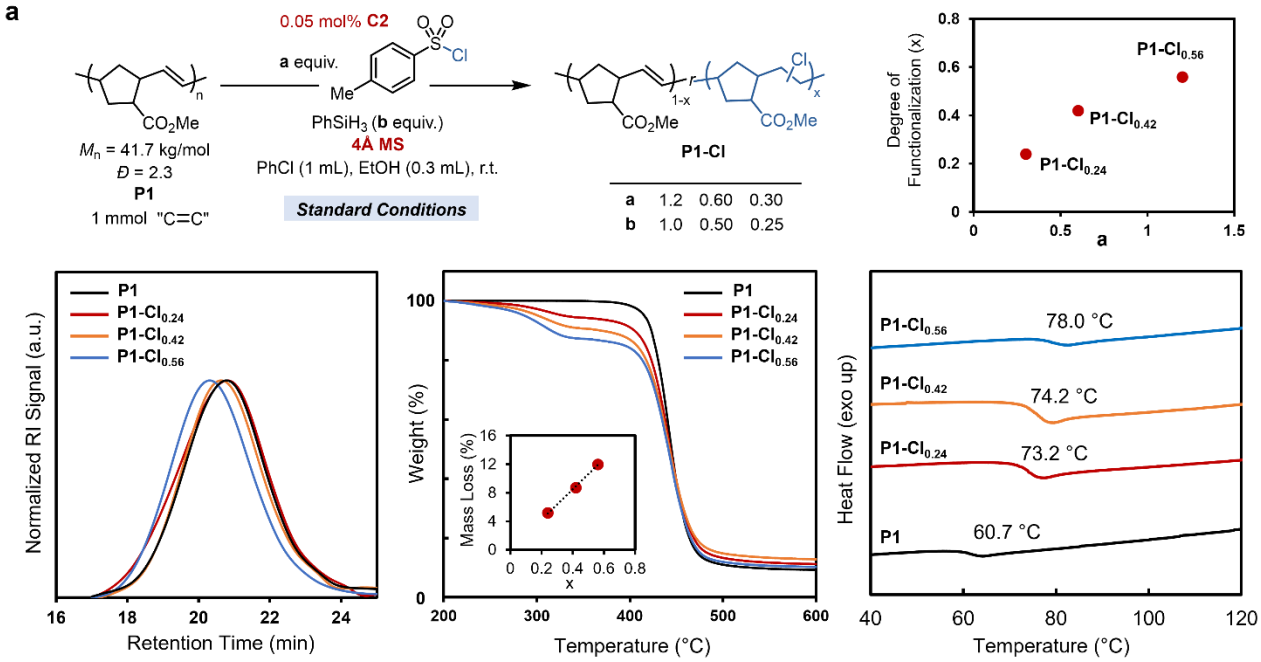

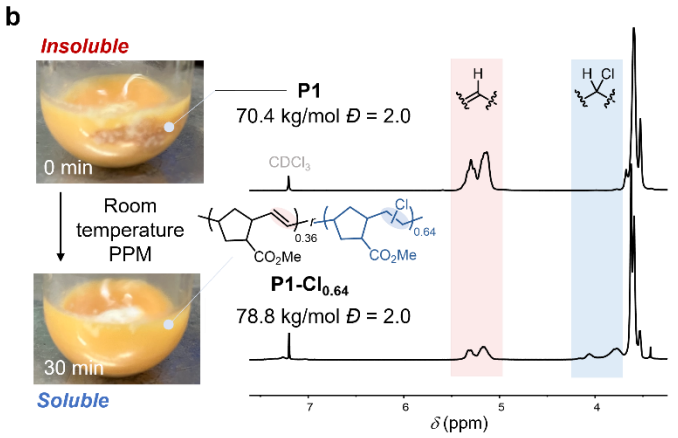

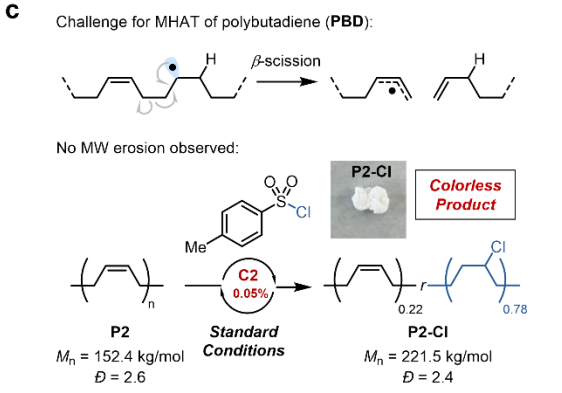

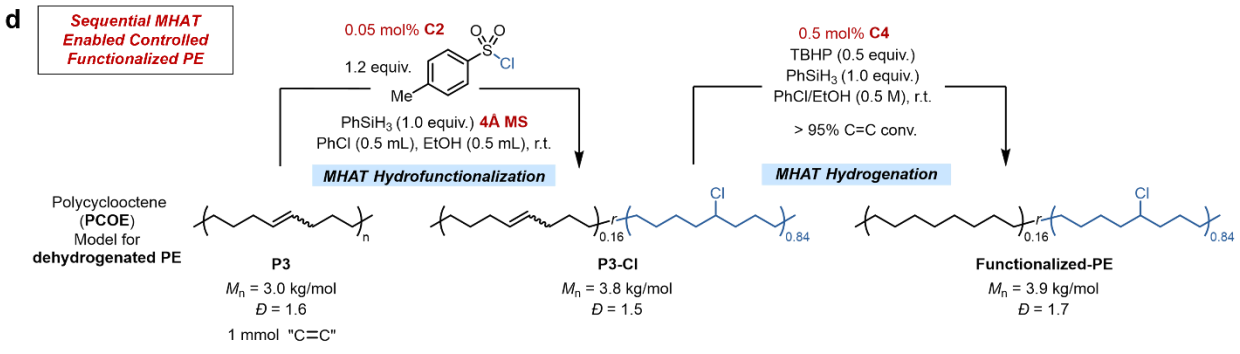

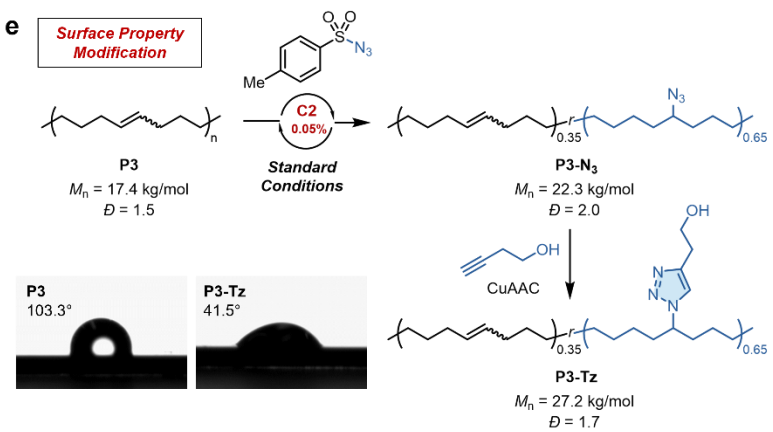

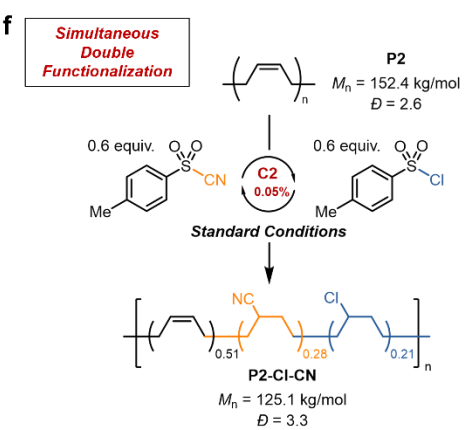

Figure 5 | Post-polymerization functionalization (PPM) enabled by modified Carreira-type hydrofunctionalization. *Standard conditions*: 1.0 mmol "C=C", **C2** (0.05 mol%), Ts−X (1.2 mmol), $PhSiH_3$ (1.0 mmol), 4Å MS (200 mg) in 1.0 mL chlorobenzene and 0.3 mL EtOH at r.t. for 12 h. For hydroazidation, **C2** (0.5 mol%) was used. The degrees of functionalization were determined by ^1H NMR spectroscopy. M_n and $Đ$ were determined by GPC (tetrahydrofuran (THF)) relative to polystyrene standards.

Compared to polynorbornenes, less sterically hindered polymers provided higher conversions. For instance, 78% of the double bonds in polybutadiene (**P2**, 152.4 kg/mol, $Đ$ = 2.6), a commodity polymer for synthetic rubber, can be swiftly hydrochlorinated using 1.2 equivalents of tosyl chloride (Figure 5c). In this case trace amount of hydrosulfonylation was also noticed (Figure S17). Despite the potential for the nascent secondary alkyl radical generated on the backbone of polybutadiene to undergo fast β-scission to afford a stable allyl radical, no molecular weight erosion was detected.[54] Meanwhile, it is worth noting that the product remained colorless as a result of the low catalyst loading, which is a highly desired feature for potential polymer-to-polymer upcycling.

Polycyclooctene (**P3**) represents another interesting substrate (Figure 5d). It has been used as a model for dehydrogenated high density polyethylene (HDPE).[55] Under the standard conditions, an 84% degree of functionalization was obtained. Moreover, we showed that the rest of the double bonds can be hydrogenated via cobalt hydride catalysis as well.[30] Thus, a new precious-metal-free PPM approach to functionalized PE is developed, with both steps enabled by catalytic MHAT chemistry.[56] Incorporating polar groups other than halides would bestow polymers more interesting properties or downstream transformations. To this, we extended this chemistry to the radicalophiles validated in Figure 5c. A highly synthetically versatile azide group was installed (**P3-N_3**), which can then undergo CuAAC reaction to afford a PE-like material with modulated surface hydrophilicity. Finally, simultaneous introduction of two different functional groups was achieved in one-pot, and the respective degree of functionalization approximately matched the feed ratio (**P2-CN-Cl**).

To conclude, we have developed a simple modified protocol of the Carreira-type CoSalen-catalyzed hydrofunctionalization and Mukaiyama hydration reactions. The key was the inhibition of Salen backbone degradation by molecular sieves. This allowed for the highly efficient conversion of challenging, unactivated 1,2-dialkyl olefins at a low catalyst loading, with 0.05 mol% being sufficient in most cases. The MHAT regioselectivity of this type of alkenes was found to be adjustable by the allylic substituents in both directions (β:γ from 6.5:1 to < 1:20), implying that radical philicity and hyperconjugation are two important controlling factors. Interesting elimination pathways associated with γ-HAT were also identified. This method also offers a unique venue for the selective, efficient, and versatile post-polymerization functionalization of commodity-relevant olefin-containing polymers. We expect these new findings to aid in the future development of related redox-neutral transformations and add to the understanding of MHAT mechanisms.

References:

1. Crossley, S. W.; Obradors, C.; Martinez, R. M.; Shenvi, R. A., Mn-, Fe-, and Co-catalyzed radical hydrofunctionalizations of olefins. *Chem. Rev.* **2016**, *116*, 8912-9000.
2. Shevick, S. L.; Wilson, C. V.; Kotesova, S.; Kim, D.; Holland, P. L.; Shenvi, R. A., Catalytic hydrogen atom transfer to alkenes: a roadmap for metal hydrides and radicals. *Chem. Sci.* **2020**, *11*, 12401-12422.
3. Isayama, S.; Mukaiyama, T., A new method for preparation of alcohols from olefins with molecular oxygen and phenylsilane by the use of bis(acetylacetonato)cobalt(II). *Chem. Lett.* **1989**, *18*, 1071-1074.
4. Zombeck, A.; Hamilton, D. E.; Drago, R. S., Novel catalytic oxidations of terminal olefins by cobalt(II)-schiff base complexes. *J. Am. Chem. Soc.* **1982**, *104*, 6782-6784.
5. Waser, J.; Carreira, E. M., Convenient synthesis of alkylhydrazides by the cobalt-catalyzed hydrohydrazination reaction of olefins and azodicarboxylates. *J. Am. Chem. Soc.* **2004**, *126*, 5676-5677.
6. Waser, J.; Nambu, H.; Carreira, E. M., Cobalt-catalyzed hydroazidation of olefins: convenient access to alkyl azides. *J. Am. Chem. Soc.* **2005**, *127*, 8294-8295.
7. Gaspar, B.; Carreira, E. M., Mild cobalt-catalyzed hydrocyanation of olefins with tosyl cyanide. *Angew. Chem. Int. Ed.* **2007**, *46*, 4519-4522.
8. Gaspar, B.; Carreira, E. M., Catalytic hydrochlorination of unactivated olefins with para-toluenesulfonyl chloride. *Angew. Chem. Int. Ed.* **2008**, *47*, 5758-5760.
9. Gaspar, B.; Carreira, E. M., Cobalt catalyzed functionalization of unactivated alkenes: regioselective reductive C-C bond forming reactions. *J. Am. Chem. Soc.* **2009**, *131*, 13214-13215.
10. Green, S. A.; Matos, J. L.; Yagi, A.; Shenvi, R. A., Branch-selective hydroarylation: iodoarene-olefin cross-coupling. *J. Am.*

Chem. Soc. **2016**, *138*, 12779-12782.
11. Ma, X.; Dang, H.; Rose, J. A.; Rablen, P.; Herzon, S. B., Hydroheteroarylation of unactivated alkenes using *N*-methoxyheteroarenium salts. *J. Am. Chem. Soc.* **2017**, *139*, 5998-6007.
12. Mayerhofer, V. J.; Lippolis, M.; Teskey, C. J., Dual-catalysed intermolecular reductive coupling of dienes and ketones. *Angew. Chem. Int. Ed.* **2024**, 63, e20231487.
13. Shigehisa, H.; Aoki, T.; Yamaguchi, S.; Shimizu, N.; Hiroya, K., Hydroalkoxylation of unactivated olefins with carbon radicals and carbocation species as key intermediates. *J. Am. Chem. Soc.* **2013**, *135*, 10306-10309.
14. Touney, E. E.; Foy, N. J.; Pronin, S. V., Catalytic radical-polar crossover reactions of allylic alcohols. *J. Am. Chem. Soc.* **2018**, *140*, 16982-16987.
15. Zhou, X. L.; Yang, F.; Sun, H. L.; Yin, Y. N.; Ye, W. T.; Zhu, R., Cobalt-catalyzed intermolecular hydrofunctionalization of alkenes: evidence for a bimetallic pathway. *J. Am. Chem. Soc.* **2019**, *141*, 7250-7255.
16. Ebisawa, K.; Izumi, K.; Ooka, Y.; Kato, H.; Kanazawa, S.; Komatsu, S.; Nishi, E.; Shigehisa, H., Catalyst- and silane-controlled enantioselective hydrofunctionalization of alkenes by cobalt-catalyzed hydrogen atom transfer and radical-polar crossover. *J. Am. Chem. Soc.* **2020**, *142*, 13481-13490.
17. Zhang, Q.; Qin, T.; Lv, G.; Meng, Q.; Zhang, G.; Xiong, T., Cobalt-catalyzed radical hydroamination of alkenes with *N*-fluorobenzenesulfonimides. *Angew. Chem. Int. Ed.* **2021**, *60*, 25949–25957.
18. Wilson, C. V.; Kim, D.; Sharma, A.; Hooper, R. X.; Poli, R.; Hoffman, B. M.; Holland, P. L., Cobalt–carbon bonding in a salen-supported cobalt(IV) alkyl complex postulated in oxidative MHAT catalysis. *J. Am. Chem. Soc.* **2022**, *144*, 10361–10367.
19. Ye, W.-T.; Zhu, R., Dioxygen-promoted cobalt-catalyzed oxidative hydroamination using unactivated alkenes and free amines. *Chem Catal.* **2022**, *2*, 345-357.
20. Wilson, C. V.; Holland, P. L., Mechanism of alkene hydrofunctionalization by oxidative cobalt(salen) catalyzed hydrogen atom transfer. *J. Am. Chem. Soc.* **2024**, *146*, 2685–2700.
21. Yang, F.; Nie, Y.-C.; Liu, H.-Y.; Zhang, L.; Mo, F.; Zhu, R., Electrocatalytic oxidative hydrofunctionalization reactions of alkenes via Co(II/III/IV) cycle. *ACS Catal.* **2022**, *12*, 2132-2137.
22. Gnaim, S.; Bauer, A.; Zhang, H.-J.; Chen, L.; Gannett, C.; Malapit, C. A.; Hill, D. E.; Vogt, D.; Tang, T.; Daley, R. A.; Hao, W.; Zeng, R.; Quertenmont, M.; Beck, W. D.; Kandahari, E.; Vantourout, J. C.; Echeverria, P.-G.; Abruna, H. D.; Blackmond, D. G.; Minteer, S. D.; Reisman, S. E.; Sigman, M. S.; Baran, P. S., Cobalt-electrocatalytic HAT for functionalization of unsaturated C–C bonds. *Nature* **2022**, *605*, 687-695.
23. Boucher, D. G.; Pendergast, A. D.; Wu, X.; Nguyen, Z. A.; Jadhav, R. G.; Lin, S.; White, H. S.; Minteer, S. D., Unraveling hydrogen atom transfer mechanisms with voltammetry: oxidative formation and reactivity of cobalt hydride. *J. Am. Chem. Soc.* **2023**, *145*, 17665–17677.
24. Park, S. H.; Bae, G.; Choi, A.; Shin, S.; Shin, K.; Choi, C. H.; Kim, H., Electrocatalytic access to azetidines via intramolecular allylic hydroamination: scrutinizing key oxidation steps through electrochemical kinetic analysis. *J. Am. Chem. Soc.* **2023**, *145*, 15360–15369.
25. Lindner, H.; Amberg, W. M.; Martini, T.; Fischer, D. M.; Moore, E.; Carreira, E. M., Photo- and cobalt-catalyzed synthesis of heterocycles via cycloisomerization of unactivated olefins. *Angew. Chem. Int. Ed.* **2024**, e202319515.
26. Kamei, Y.; Seino, Y.; Yamaguchi, Y.; Yoshino, T.; Maeda, S.; Kojima, M.; Matsunaga, S., Silane- and peroxide-free hydrogen atom transfer hydrogenation using ascorbic acid and cobalt-photoredox dual catalysis. *Nat. Commun.* **2021**, *12*, 966.
27. Nakagawa, M.; Matsuki, Y.; Nagao, K.; Ohmiya, H., A triple photoredox/cobalt/Brønsted acid catalysis enabling Markovnikov hydroalkoxylation of unactivated alkenes. *J. Am. Chem. Soc.* **2022**, *144*, 7953–7959.
28. Liu, J.; Rong, J.; Wood, D. P.; Wang, Y.; Liang, S. H.; Lin, S., Co-catalyzed hydrofluorination of alkenes: photocatalytic method development and electroanalytical mechanistic investigation. *J. Am. Chem. Soc.* **2024**, *146*, 4380–4392.
29. Iwasaki, K.; Wan, K. K.; Oppedisano, A.; Crossley, S. W.; Shenvi, R. A., Simple, chemoselective hydrogenation with thermodynamic stereocontrol. *J. Am. Chem. Soc.* **2014**, *136*, 1300-1303.
30. Ma, X.; Herzon, S. B., Non-classical selectivities in the reduction of alkenes by cobalt-mediated hydrogen atom transfer. *Chem. Sci.* **2015**, *6*, 6250-6255.
31. Li, G.; Shi, S.; Qian, J.; Norton, J. R.; Xu, G.-X.; Liu, J.-R.; Hong, X., Kinetics of H· transfer from $CpCr(CO)_3H$ to various enamides: application to construction of pyrrolidines. *JACS Au* **2023**, *3*, 3366-3373.
32. Crossley, S. W.; Barabe, F.; Shenvi, R. A., Simple, chemoselective, catalytic olefin isomerization. *J. Am. Chem. Soc.* **2014**, *136*, 16788-16791.
33. Li, G.; Kuo, J. L.; Han, A.; Abuyuan, J. M.; Young, L. C.; Norton, J. R.; Palmer, J. H., Radical isomerization and cycloisomerization initiated by H· transfer. *J. Am. Chem. Soc.* **2016**, *138*, 7698-7704.
34. Herbort, J. H.; Bednar, T. N.; Chen, A. D.; RajanBabu, T. V.; Nagib, D. A., γ C-H Functionalization of amines via triple H-atom transfer of a vinyl sulfonyl radical chaperone. *J. Am. Chem. Soc.* **2022**, *144*, 13366-13373.
35. Yin, Y. N.; Ding, R. Q.; Ouyang, D. C.; Zhang, Q.; Zhu, R., Highly chemoselective synthesis of hindered amides via cobalt-catalyzed intermolecular oxidative hydroamidation. *Nat. Commun.* **2021**, *12*, 2552.
36. Huang, L.; Arndt, M.; Goossen, K.; Heydt, H.; Goossen, L. J., Late transition metal-catalyzed hydroamination and hydroamidation. *Chem. Rev.* **2015**, *115*, 2596-2697.
37. Xi, Y.; Ma, S.; Hartwig, J. F., Catalytic asymmetric addition of an amine N-H bond across internal alkenes. *Nature* **2020**, *588*, 254-260.
38. Yang, Y.; Shi, S. L.; Niu, D.; Liu, P.; Buchwald, S. L., Catalytic asymmetric hydroamination of unactivated internal olefins to aliphatic amines. *Science* **2015**, *349*, 62-66.

39. Menendez Rodriguez, G.; Díaz-Requejo, M. M.; Pérez, P. J., Metal-catalyzed postpolymerization strategies for polar group incorporation into polyolefins containing C–C, C=C, and aromatic rings. *Macromolecules* **2021**, *54*, 4971-4985.
40. Gitter, S.; Teh, W. P.; Yang, X.; Dohoda, A.; Michael, F.; Boydston, A. J., C-H Functionalization and allylic amination for post-polymerization modification of polynorbornenes. *Angew. Chem. Int. Ed.* **2023**, *62*, e202303174.
41. Saito, T.; Hill, M. R.; Lennon Luo, S.-X.; Ye, H.-Z.; Van Voorhis, T.; Johnson, J. A., Converting commodity polyolefins to electronic materials through borane-catalyzed alkene isomerization. *J. Am. Chem. Soc.* **2022**, *144*, 23010–23018.
42. Scott, S. S.; Kaur, B.; Zheng, C. H. M.; Brant, P.; Gilmour, D. J.; Schafer, L. L., Amine-functionalized polybutadiene synthesis by tunable postpolymerization hydroaminoalkylation. *J. Am. Chem. Soc.* **2023**, *145*, 22871-22877.
43. Chen, Z.; Brookhart, M., Exploring ethylene/polar vinyl monomer copolymerizations using Ni and Pd α-diimine catalysts. *Acc. Chem. Res.* **2018**, *51*, 1831-1839.
44. Zhang, Z.; Zhang, Y.; Zeng, R., Photoinduced iron-catalyzed C-H alkylation of polyolefins. *Chem. Sci.* **2023**, *14*, 9374-9379.
45. Demarteau, J.; Debuigne, A.; Detrembleur, C., Organocobalt complexes as sources of carbon-centered radicals for organic and polymer chemistries. *Chem. Rev.* **2019**, *119*, 6906–6955.
46. Matos, J. L. M.; Green, S. A.; Chun, Y.; Dang, V. Q.; Dushin, R. G.; Richardson, P.; Chen, J. S.; Piotrowski, D. W.; Paegel, B. M.; Shenvi, R. A., Cycloisomerization of olefins in water. *Angew. Chem. Int. Ed.* **2020**, *59*, 12998-13003.
47. Hell, Z.; Magyar, Á.; Juhász, K., The application of 4Å molecular sieves in organic chemical syntheses: an overview. *Synthesis* **2020**, *53*, 279-295.
48. Waser, J.; Gaspar, B.; Nambu, H.; Carreira, E. M., Hydrazines and azides via the metal-catalyzed hydrohydrazination and hydroazidation of olefins. *J. Am. Chem. Soc.* **2006**, *128*, 11693-11712.
49. Schrauzer, G. N.; Windgassen, R. J., On hydroxyalkylcobaloximes and the mechanism of a cobamide-dependent diol dehydrase. *J. Am. Chem. Soc.* **1967**, *89*, 143-147.
50. See S29 for detail.
51. Santiago, C. B.; Guo, J. Y.; Sigman, M. S., Predictive and mechanistic multivariate linear regression models for reaction development. *Chem. Sci.* **2018**, *9*, 2398-2412.
52. Leah, D. G.-O. N.; Alcindor, F. B.; Terry, L. M.; Brian, G. P., Calculating group electronegativities using the revised Lewis–Langmuir equation. *J. Mol. Struc: THEOCHEM* **2003**, *639*, 151-156.
53. Wang, X.; Wilson, T. J.; Alentiev, D.; Gringolts, M.; Finkelshtein, E.; Bermeshev, M.; Long, B. K., Substituted polynorbornene membranes: a modular template for targeted gas separations. *Polym. Chem.* **2021**, *12*, 2947-2977.
54. Moad, G., The synthesis of polyolefin graft copolymers by reactive extrusion. *Prog. Polym. Sci.* **1999**, *24*, 81-142.
55. Chethalen, R. J.; Fastow, E. J.; Coughlin, E. B.; Winey, K. I., Thiol-ene click chemistry incorporates hydroxyl functionality on polycyclooctene to tune properties. *ACS Macro. Lett.* **2023**, *12*, 107-112.
56. Chaudhry, A. U.; Mittal, V., Blends of high-density polyethylene with chlorinated polyethylene: morphology, thermal, rheological, and mechanical properties. *Polym. Eng. Sci.* **2014**, *54*, 85-95.

Acknowledgments

Financial support was provided by the Natural Science Foundation of China (22222101, 22350006 and 22171012), Beijing Natural Science Foundation (2242006), and BNLMS. Computation was supported by high-performance computing platform of Peking University. B.-S.Z. acknowledges the Beijing Natural Science Foundation (QY23028) for supporting undergraduate research. The authors would like to thank Prof. Bingjun Xu and Qiwen Sun (PKU) for GC-FID instrumentation.

Author contributions

R.Z. proposed the transformation. Y.-N.Y., B.-S.Z., H.-Y.L., R.-Q.S. and D.-C.O conducted the experimental investigation. R.Z., Y.-N.Y. and B.-S.Z. wrote the manuscript.

Competing interests

The authors declare no competing interests.

Corresponding author

Correspondence to Rong Zhu.

Data availability

The data supporting the findings of this study are available within the article and its Supplementary Materials. Additional data are available from the corresponding author upon request.